Supplementary Information

Origin of flaw-tolerance in nacre

Zaiwang Huang[1] & Xiaodong Li[1]

[1]Department of Mechanical Engineering, University of South Carolina, 300 Main Street, Columbia, South Carolina 29208, USA.

Correspondence and requests for materials should be addressed to X. L. (lixiao@cec.sc.edu).

1. **Experimental procedure for peeling-off technique.**
2. **XRD determination of single-crystal geologic aragonite mineral.**
3. **AFM observation for crack propagation along grain boundary of aragonite nanoparticles.**
4. **TEM observation for the roughness of biopolymer interlayer.**
5. **Nanoindentation loading function outfitted with cube-corner nanoindenter**
6. **SEM observation of synthesized pure aragonite rod.**
7. **AFM observation for nanoparticle architecture from indented and un-indented areas using Vickers indentation.**

1. Experimental procedure for peeling-off technique.

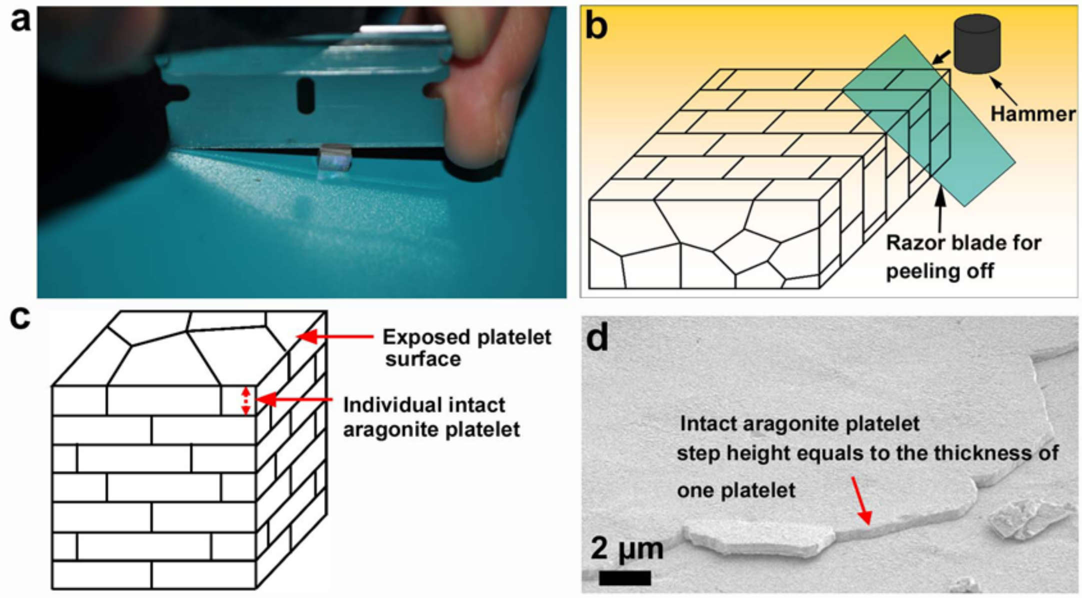

Figure S1 | Preparation for platelet surface using peeling-off method. **a**, A razor blade was used to peel off the nacre specimen along cross section. **b**, A schematic showing experimental details **c**, Owing to the weak biopolymer interface, this peeling-off process will completely split the specimen along interface, thus, the exposed layer at the top surface will be the intact aragonite platelet. This guarantees that the indented depth for nanoindentation is restrictedly within individual aragonite platelet, avoiding the effect from biopolymer layer. It is almost impossible to prepare such a sample using crystallographic grinding/polishing. **d**, Typical SEM observation for the top surface after peeling-off.

2. XRD determination of single-crystal geologic aragonite mineral.

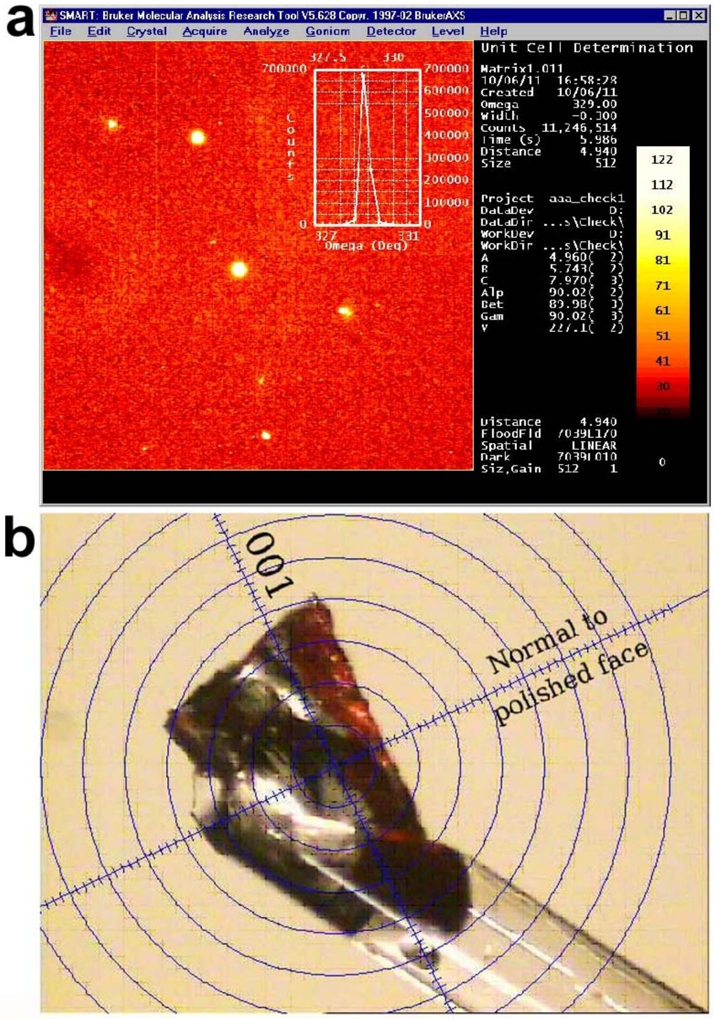

Figure S2 │ XRD measurement of geologic aragonite mineral using a Bruker SMART APEX diffractometer equipped with Mo K radiation, λ= 0.71073 Å). **a**, One X-ray diffraction data frame and the peak profile of a representative peak (inset). The crystal system was determined to be primitive orthorhombic with a=4.960(2) Å, b = 5.743(2) Å, c = 7.970(3) Å. **b**, The polished plane parallel with the pristine hexagonal surface was marked with red ink. Through using the face-indexing mode of the diffractometer, the indices of the polished face were determined to be (001), indexed to the unit cell given above.

3. AFM observation for crack propagation along grain boundary of aragonite nanoparticles.

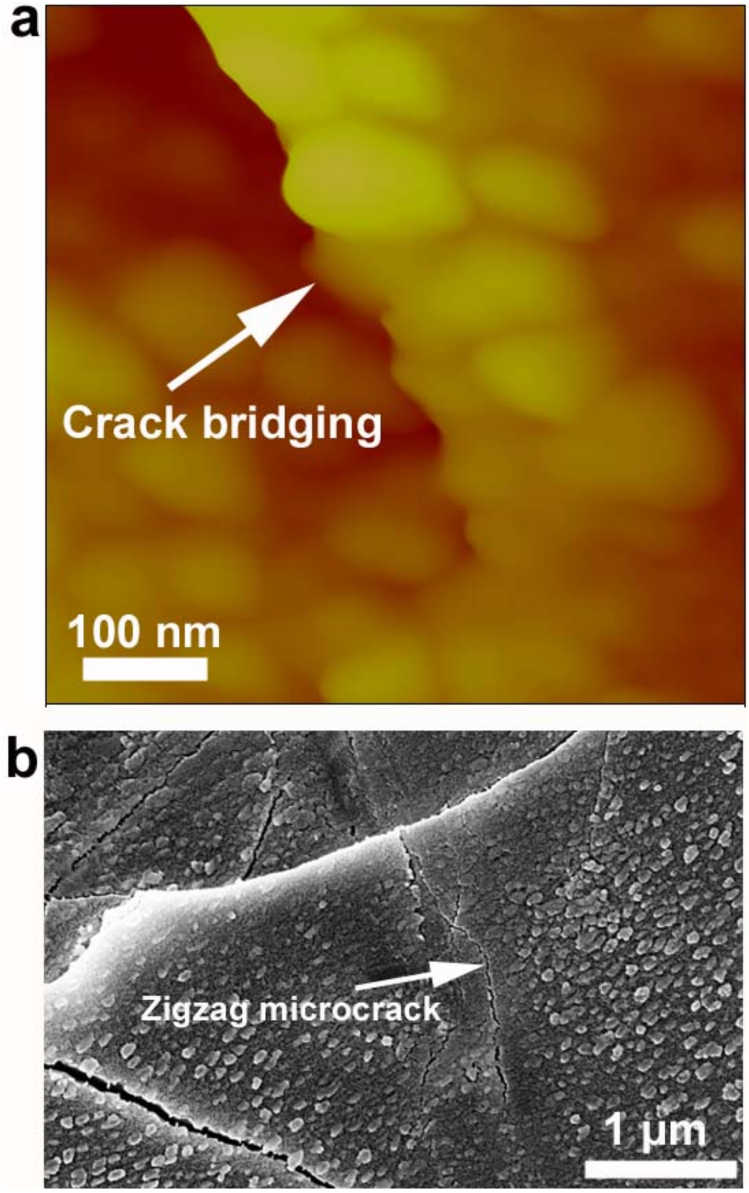

Figure S3 │ Crack profile observation within individual aragonite platelet, the cracks initiated by Vickers indentation. **a**, A crack propagates along grain boundary of nanoparticles and terminates inside an aragonite platelet. **b**, SEM observation shows, besides main crack, that microcrack can be initiated within individual aragonite platelet in a zigzag manner, implying extension resistance from inherent microstructure.

4. TEM observation for the roughness of biopolymer interlayer.

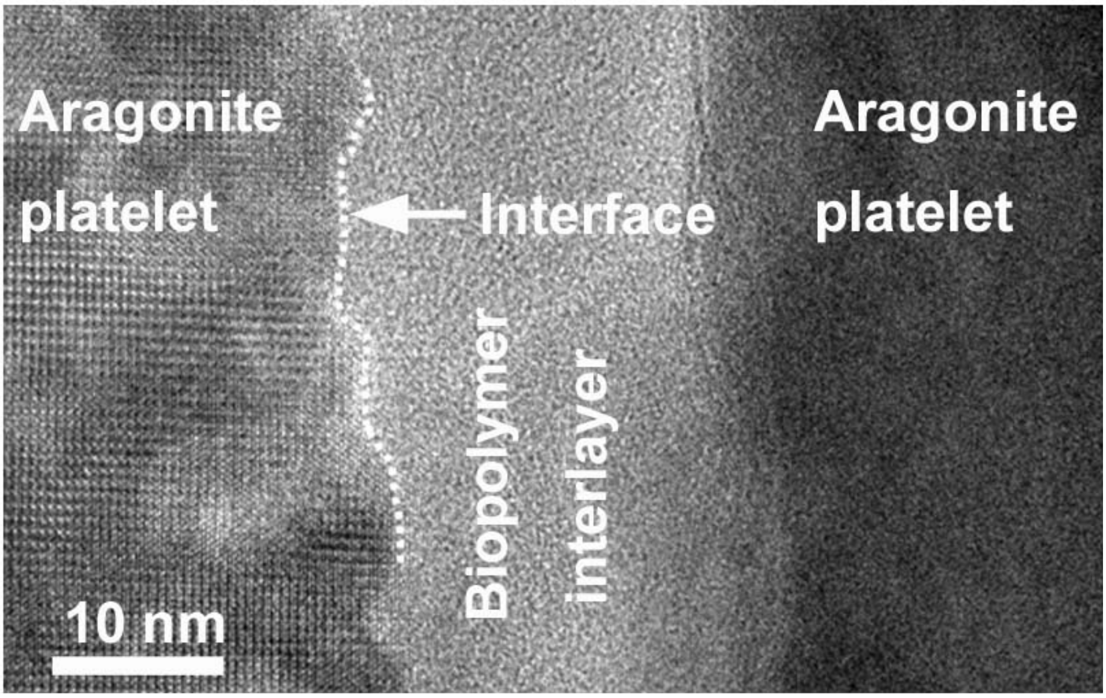

Figure S4 │ TEM micrograph of the interface of aragonite platelet and biopolymer interlayer. The atomically sharp interface shows relatively flat profile, which is in sharp contrast with bumpy edge with an amplitude of a few nanometers in Figure 2c.

5. Nanoindentation loading function outfitted with cube-corner nanoindenter

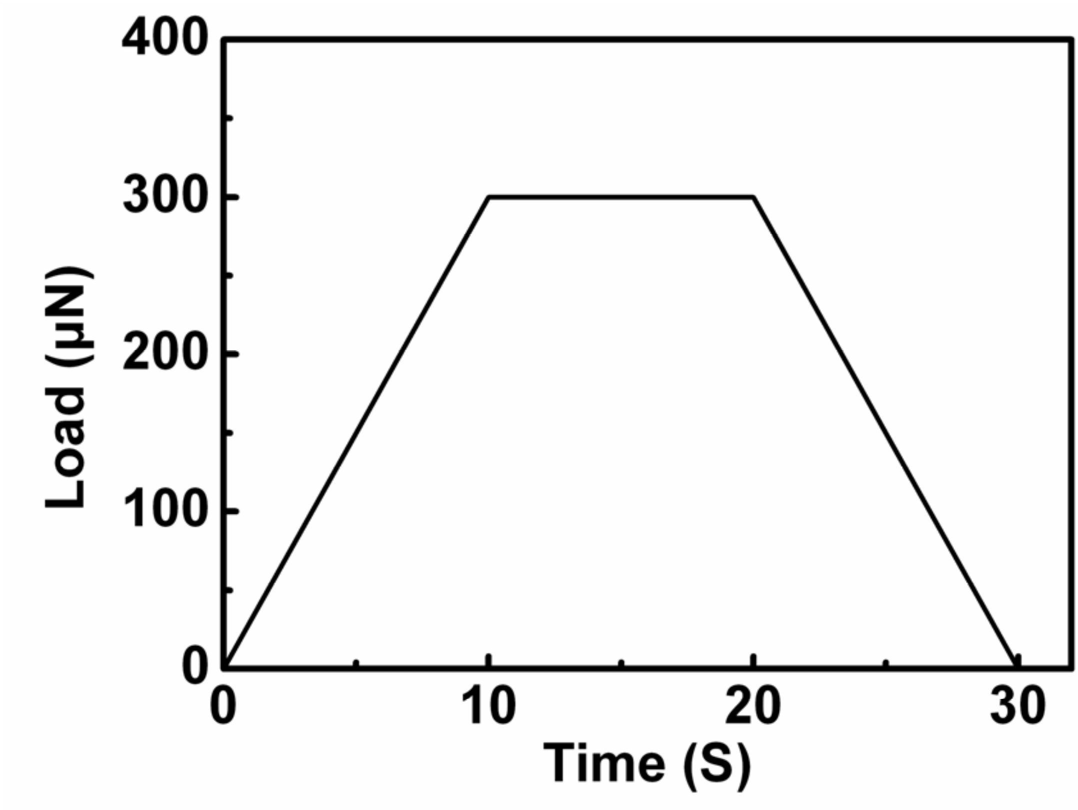

Figure S5 │ Loading function for nanoindentation outfitted with cube-corner nanoindenter. The corresponding time for loading, holding, and unloading are 10 seconds, respectively.

6. SEM observation of synthesized pure aragonite rod.

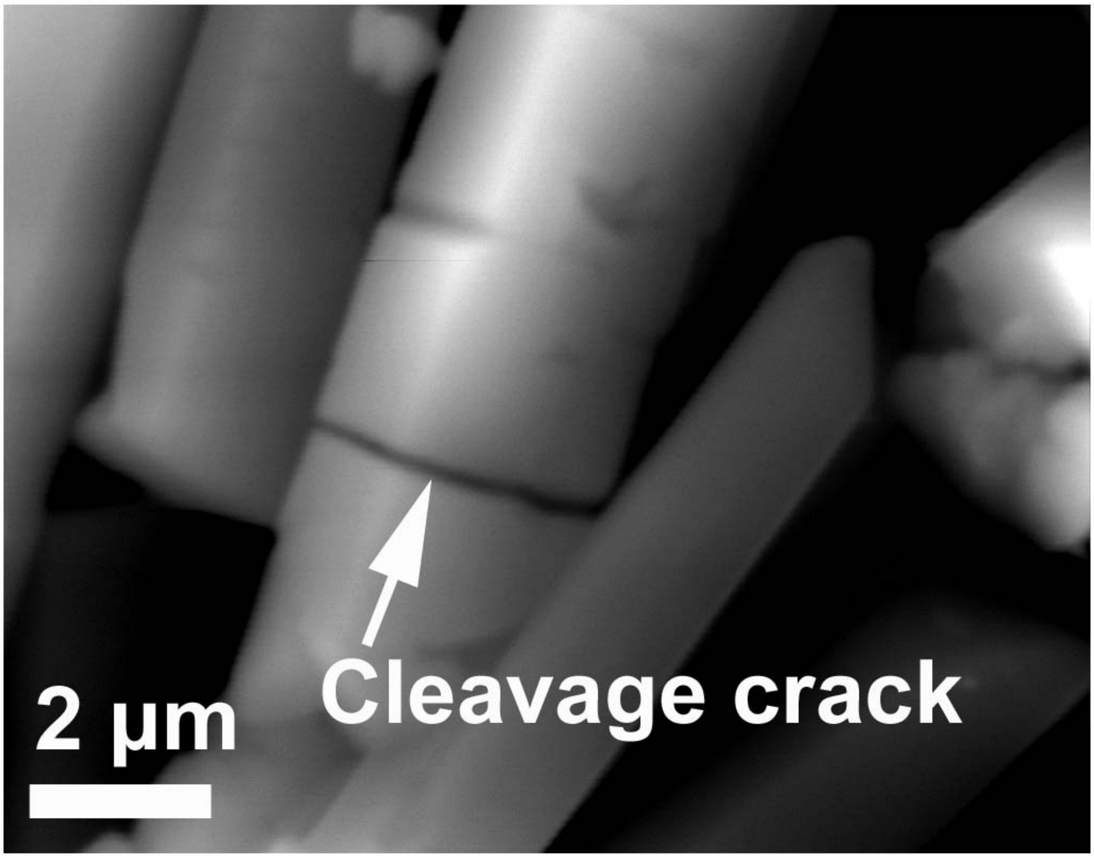

Figure S6 │ Crack failure observation in synthesized pure aragonite rod (Reference S1). The average diameter of synthesized aragonite rod is on the order of several microns. After finger-print, some micro-size rods failed and exhibit brittle fracture manner. This SEM micrograph shows typical cleavage crack profile.

7. AFM observation for nanoparticle architecture from indented and un-indented areas using Vickers indentation.

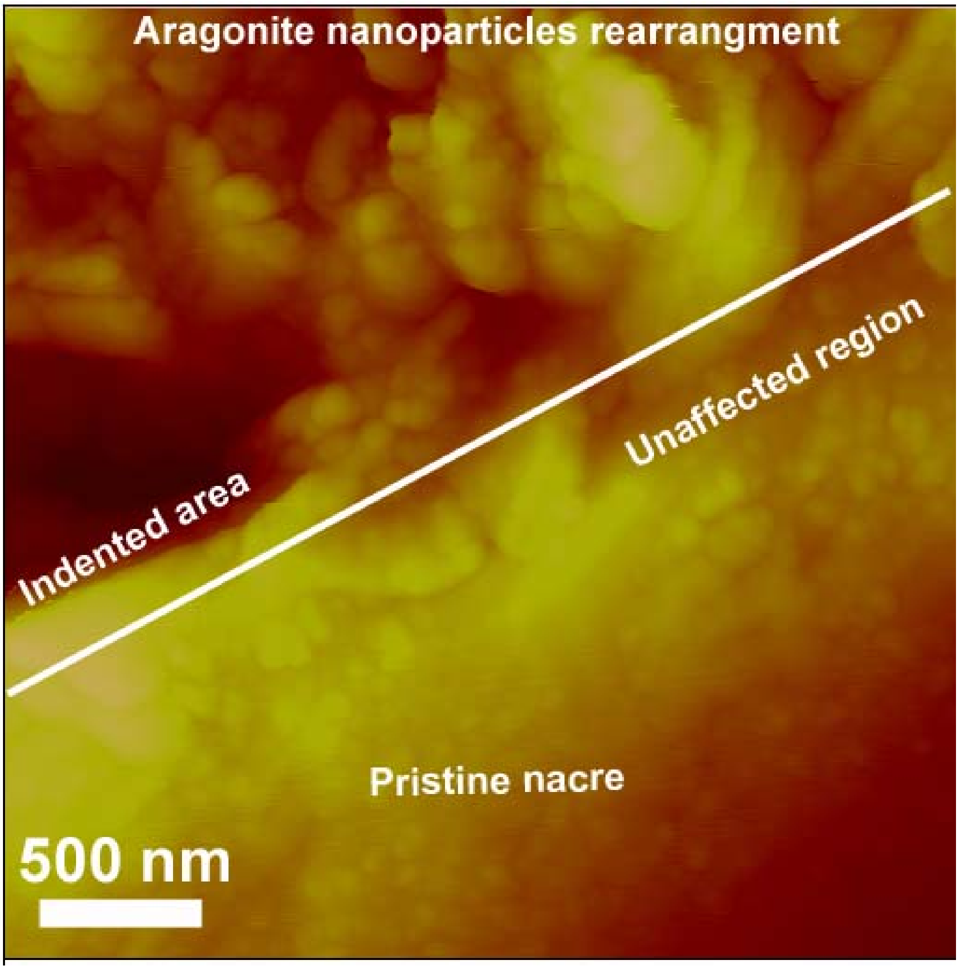

Figure S7 │ Remarkable contrast AFM observation for nanoparticle architecture. After Vickers indentation under 200 μN (holding time 15 seconds) was applied on the platelet surface (along [002]). On the indented area, the well-packed aragonite nanoparticles from pristine nacre have been severely indented in a disordered manner, exhibiting creep-like deformation behavior. In contrast, for the un-contacted area, the architecture persists.

References

S1. M. S. Rao, S. R. Yoganarasimhan, Am. Mineral. **50**, 1489 (1965).